

Fast, low-cost preparation of hackmanite minerals with reversible photochromic behavior using a microwave-assisted structure-conversion method

José M. Carvalho,^a Isabella Norrbo,^b Rômulo A. Ando,^c Hermi F. Brito,^c Márcia C.A. Fantini,^a and Mika Lastusaari,^{b,d,*}

^a University of São Paulo, Institute of Physics, 05508-000, São Paulo-SP, Brazil.

^b University of Turku, Department of Chemistry, FI-20014 Turku, Finland.

^c University of São Paulo, Institute of Chemistry, 05508-000, São Paulo-SP, Brazil.

^d Turku University Centre for Materials and Surfaces (MatSurf), FI-20014 Turku, Finland.

*e-mail: miklas@utu.fi

1. Experimental part

1.1. Materials and preparation

The polycrystalline hackmanite minerals $(M,Na)_8Al_6Si_6O_{24}(Cl,S)_2$ (M:Li, Na, and K) were prepared by thoroughly mixing and grinding the starting materials : dried Zeolite A (0.7000 g, Sigma-Aldrich, product n° 96096) (**Fig. S1**), Na_2SO_4 (0.0600 g, E. Merck, 99%), NaCl (0.1175 g, J. T. Barker, 99.5%), and in order to obtain different compositions, LiCl (0.0850 g, Acros, 99%), and KCl (0.1816 g, Vetec, 99%). In a typical preparation, 14 g of granular carbon (\varnothing : 1 to 2 mm, Synth) was used as the microwave susceptor, and placed in an alumina crucible (50 cm^3). The susceptor is used to absorb the microwave radiation initially and convert it into heat. A second alumina crucible (5 cm^3) was then used to hold 0.5 g of the precursor powder mixture prepared as described above. This crucible was placed into the granular carbon surrounding the sample with a sufficient amount of susceptor, and then both crucibles were covered with an alumina lid. The two crucibles were then placed into a cavity of aluminosilicate thermal insulation bricks (**Fig. S2**). Finally, the materials were irradiated in a conventional microwave oven (Electrolux MEF41) using a previously adjusted microwave program (**Fig. S3**). The duration of irradiation and the power levels were optimized following the temperature-power dependence constructed utilizing a hand pyrometer (**Fig. S3**). The temperature of the granular carbon has a *log* dependence on the irradiation time where a plateau is achieved after the rate of heat flowing out of the system equals the rate of heat formation¹. The microwave program was determined to provide temperatures close to 850 °C (12 to 20 minutes at 400 W). After several trials, the method proved to be reproducible.

The susceptor used in the preparation provides a reducing atmosphere of CO generated from the incomplete combustion of the granular carbon. The microwave irradiation favors the formation of CO atmosphere in temperature as low as 250 °C, and after 500 °C CO is the primary gaseous component in the reactional vessel. The preferable formation of CO gas is due to the

reduction in the apparent enthalpy in the microwave-driven Boudouard reaction² ($\text{CO}_2 + \text{C} \rightleftharpoons 2 \text{CO}$). The reducing atmosphere is used to guarantee that the sulfate anion used as a precursor (Na_2SO_4) is reduced to sulfide species (S^{2-}) in the final hackmanite materials.

For the series of *ex-situ* measurements, the material's precursors were irradiated with the microwave at different periods of time (0, 2, 4, 6, 8, 10, 12, 14, 18, and 20 minutes). After the microwave irradiation, the material was quenched to room temperature and collected to further characterization.

1.2. Characterization

The crystal structure of the materials was verified with X-ray powder diffraction (XPD) measurements using a Bruker D8 Discover - DaVinci with $\text{CuK}\alpha$ radiation (1.5418 \AA) between 5 and 100 degrees (in 2θ) with 0.02 degree 2θ step and 1 s integration time per step. Rietveld refinements were performed with TOPAS 5 program suite using the fundamental parameters (FP) function profile.

Synchrotron radiation X-ray absorption spectroscopy (SR-XAS) data were collected at the beamline SXS (D04A) in the soft X-rays energy range (900 to 5500 eV) at LNLS, CNPEM, Campinas, Brazil. The data were recorded using a double crystal monochromator of Si (111) and energy resolution of $\Delta E = 0.45 \text{ eV}$. The total electron yield (TEY - Keithley electrometer, model 6514) and Fluorescence (FY - Amptek, model X123) detectors were used.

The photoluminescence spectra were registered with a HORIBA Jobin Yvon - FLUORLOG 3-11 spectrofluorometer equipped with a double-grating monochromator in the emission position (iHR320) and a Synapse HORIBA Jobin Yvon E2V CCD30 (1024x256 pixels) CCD detector. A 450 W xenon lamp was used as the irradiation source.

The photochromic behavior was observed using a hand-lamp for irradiating the sample at different periods of time. The bleaching was achieved using different sources of radiation: 405 nm (5 W) LED hand-lamp, and a 405 nm (100 mW) laser pointer.

The infrared spectra were obtained in a FT-IR Bruker Alpha spectrometer using an attenuated total reflectance accessory of single reflection (ATR with a platinum-crystal diamond). Thirty-two spectra were accumulated for each sample using a spectral resolution of 4 cm^{-1} .

The Raman spectra were obtained in a triple monochromator Horiba-Jobin-Yvon T64000 spectrometer coupled to a microscope using the $\lambda_0 = 514.5 \text{ nm}$ excitation line from a mixed Ar^+/Kr^+ Laser (Coherent, 70C). Twenty spectra of twenty seconds of integration time were accumulated using a spectral resolution of 2 cm^{-1} .

The tenebrescence properties were followed *ex-situ* after different periods of time of MW irradiation. This was done using a 5 min exposure at 254 nm with 0.35 mW/cm^2 irradiance

under 2160 lx white incandescent light. The total reflectance was obtained by integrating the area of the curve between 400 and 700 nm after subtraction of the background.

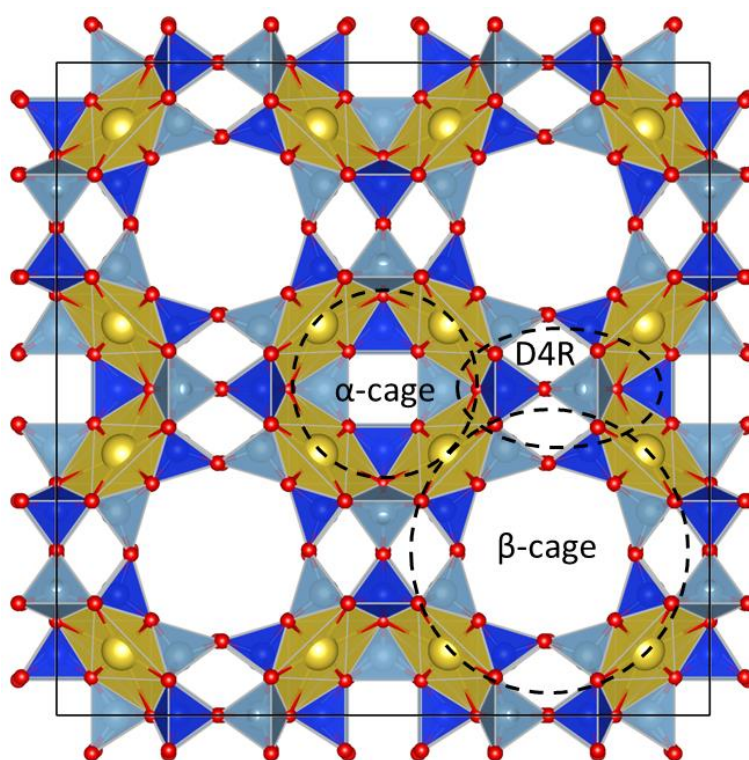


Figure S1. Structure of Na-zeolite A (PDF #04-010-2001) depicting secondary building units α -cage, β -cage (sodalite cage), and double four-membered rings (D4R). The water molecules inside the α - and β -cages are not shown for better clarity.

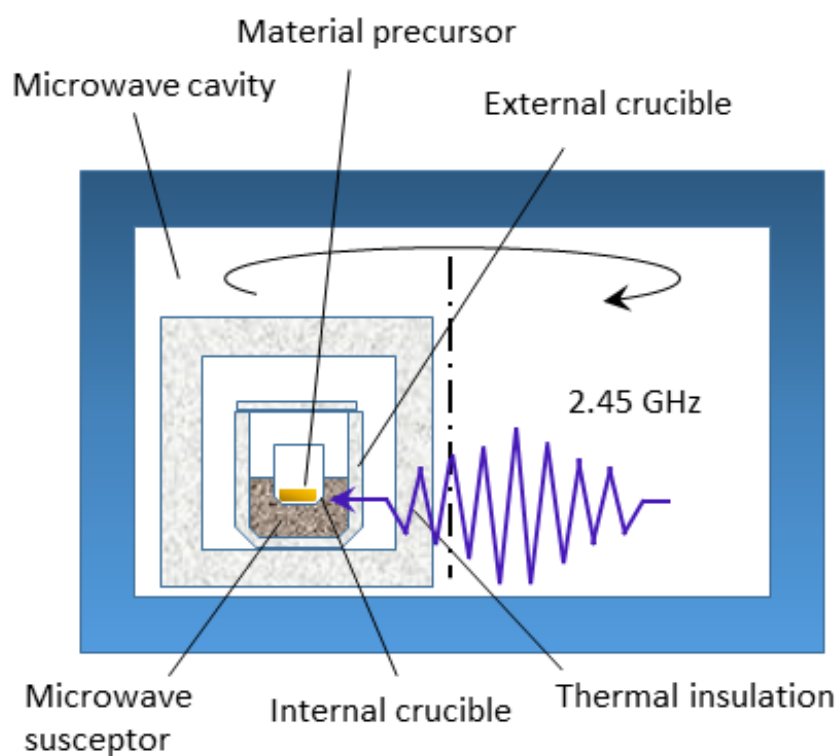


Figure S2. Microwave-assisted structure-conversion setup to synthesize the hackmanite materials. Both external and internal crucibles are made of alumina. The microwave susceptor used was granular carbon. The thermal insulation is a low-density aluminosilicate brick. All the materials were prepared in a conventional microwave oven.

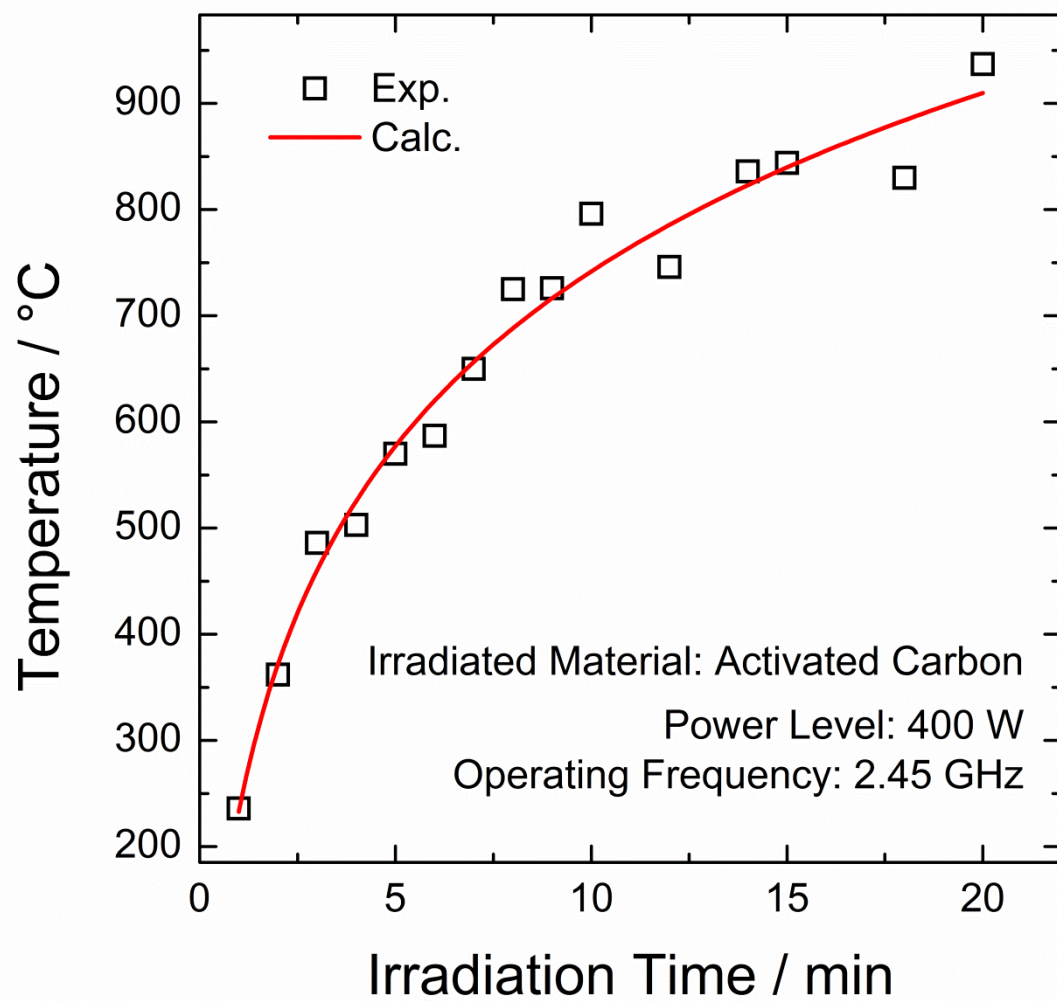


Figure S3. The temperature-time relation of the activated carbon when irradiated by microwave (frequency: 2.45 GHz) with different exposure times. The data were fitted by a conventional logarithmic growth.

Table 1. Crystal lattice parameters obtained with the Rietveld refinement for the $\text{Na}_8\text{Al}_6\text{Si}_6\text{O}_{24}(\text{Cl},\text{S})_2$ material

Structure (Space Group)	Z	a (Å)	cell volume (Å ³)	R_{Bragg}
Cubic (P-43n)	1	8.90318	705.724	2.632

Table 2. Atomic coordinates, occupations and isotropic temperature factors for the for the $\text{Na}_8\text{Al}_6\text{Si}_6\text{O}_{24}(\text{Cl},\text{S})_2$ material.

Atom	Wyckoff Position	x	y	z	Occ.	B_{iso}
Na	8e	0.17770	0.17770	0.17770	1	1.50
Al	6c	0.25000	0.00000	0.50000	1	0.80
Si	6d	0.25000	0.50000	0.00000	1	0.35
O	24i	0.16623	0.15397	0.41324	1	0.90
Cl	2a	0.00000	0.00000	0.00000	1	1.90

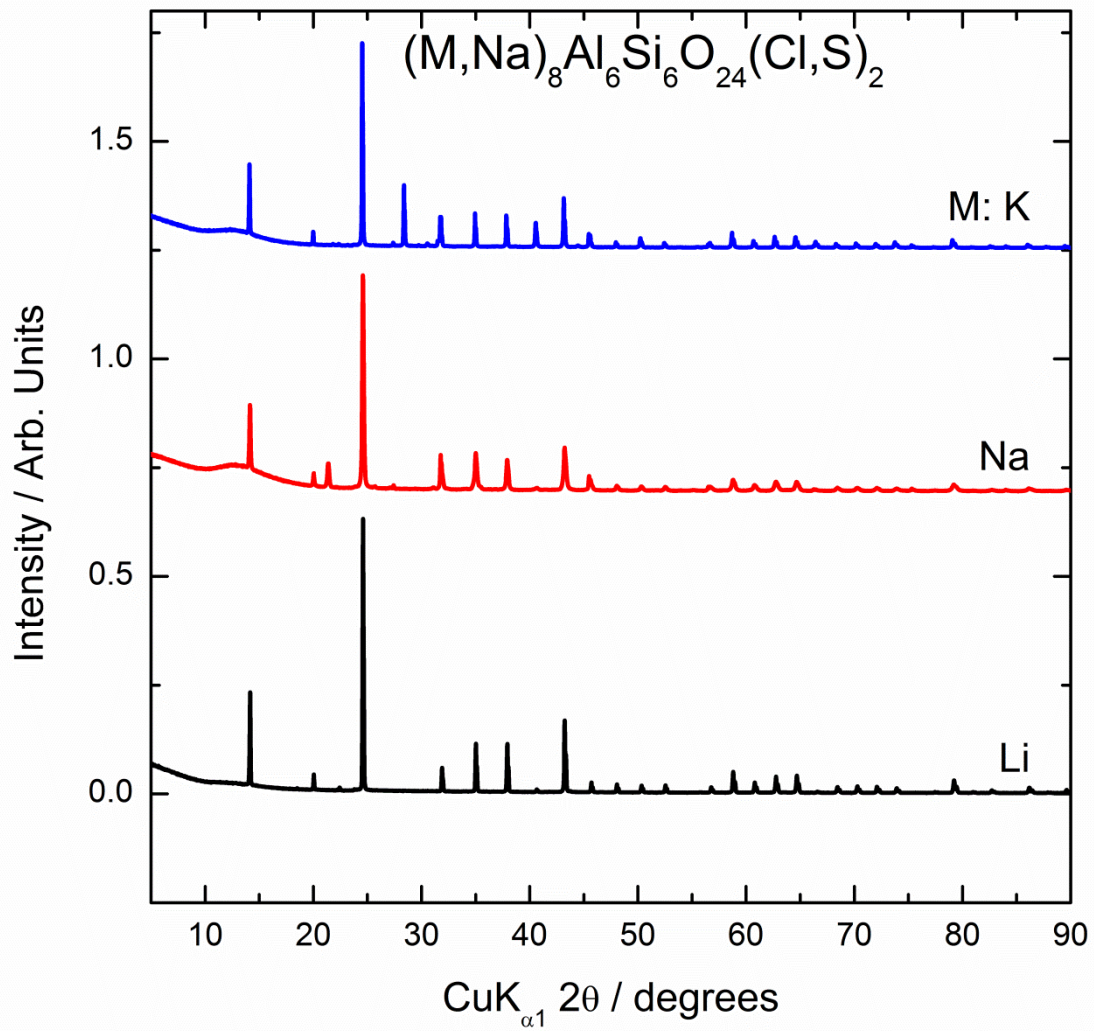


Figure S4. X-ray powder diffraction of the $(M,Na)_8$ -hackmanite materials (M: Li, Na, and K).

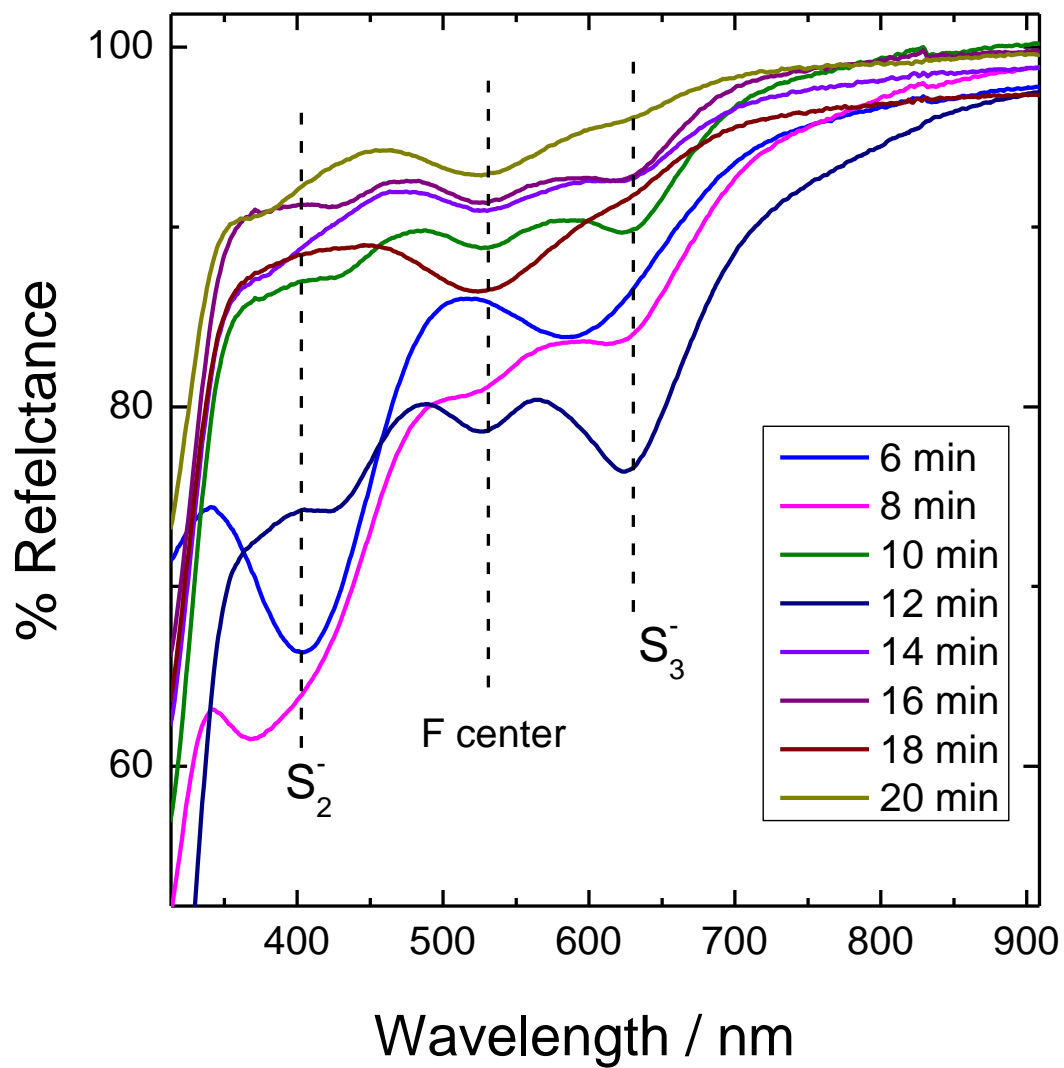


Figure S5. Photochromic response of the hackmanite materials ($\text{Na}_8\text{Al}_6\text{Si}_6\text{O}_{24}(\text{Cl},\text{S})_2$) in different steps of synthesis.

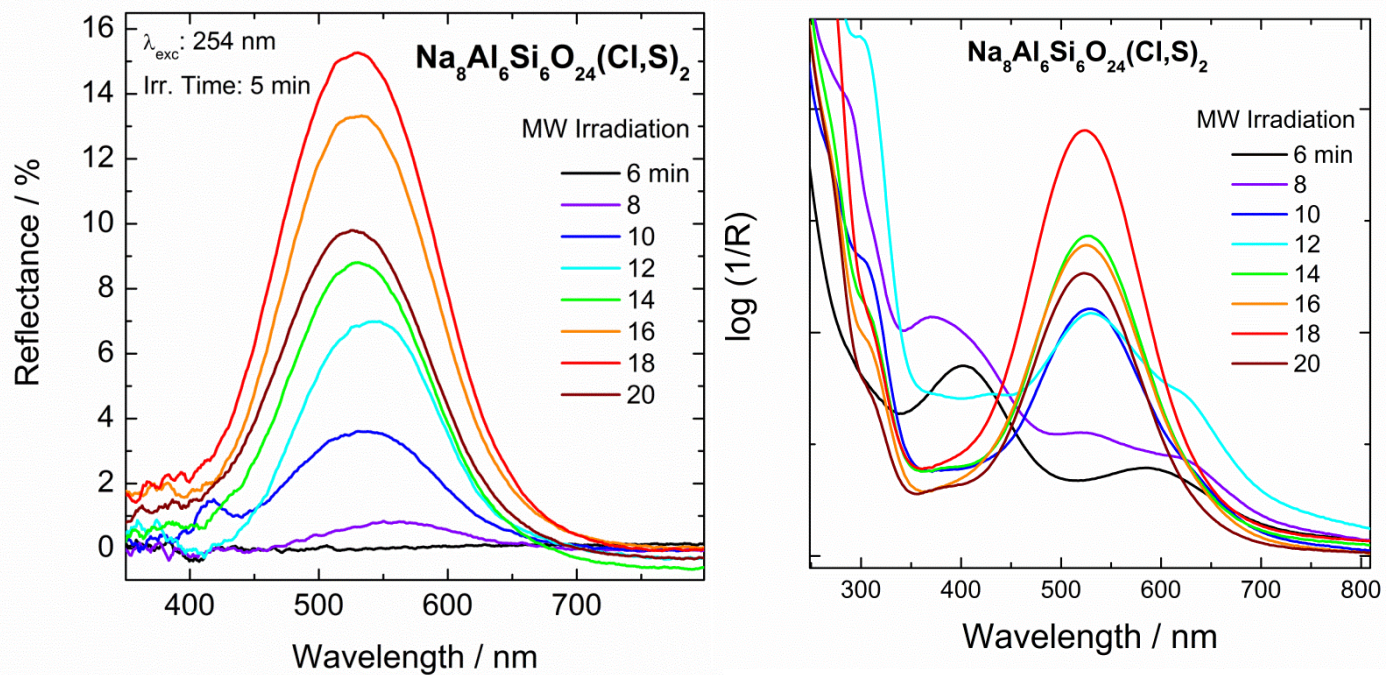


Figure S6. Corrected total reflectance (left) and absorption (right) spectra of the hackmanite materials ($\text{Na}_8\text{Al}_6\text{Si}_6\text{O}_{24}(\text{Cl},\text{S})_2$) in different time steps of synthesis.

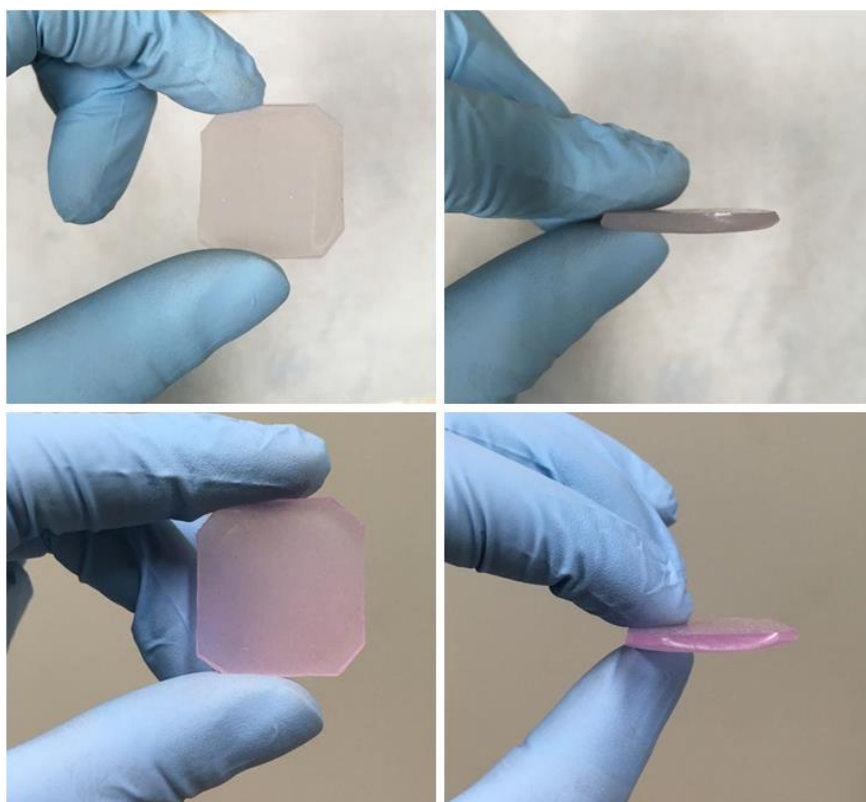


Figure S7. Hackmanite mineral obtained by MASC synthesis dispersed in a silicone polymer matrix before (top) and after (bottom) UV irradiation. The purple coloration was obtained after 5 min irradiation with hand UV-lamp (254 nm).

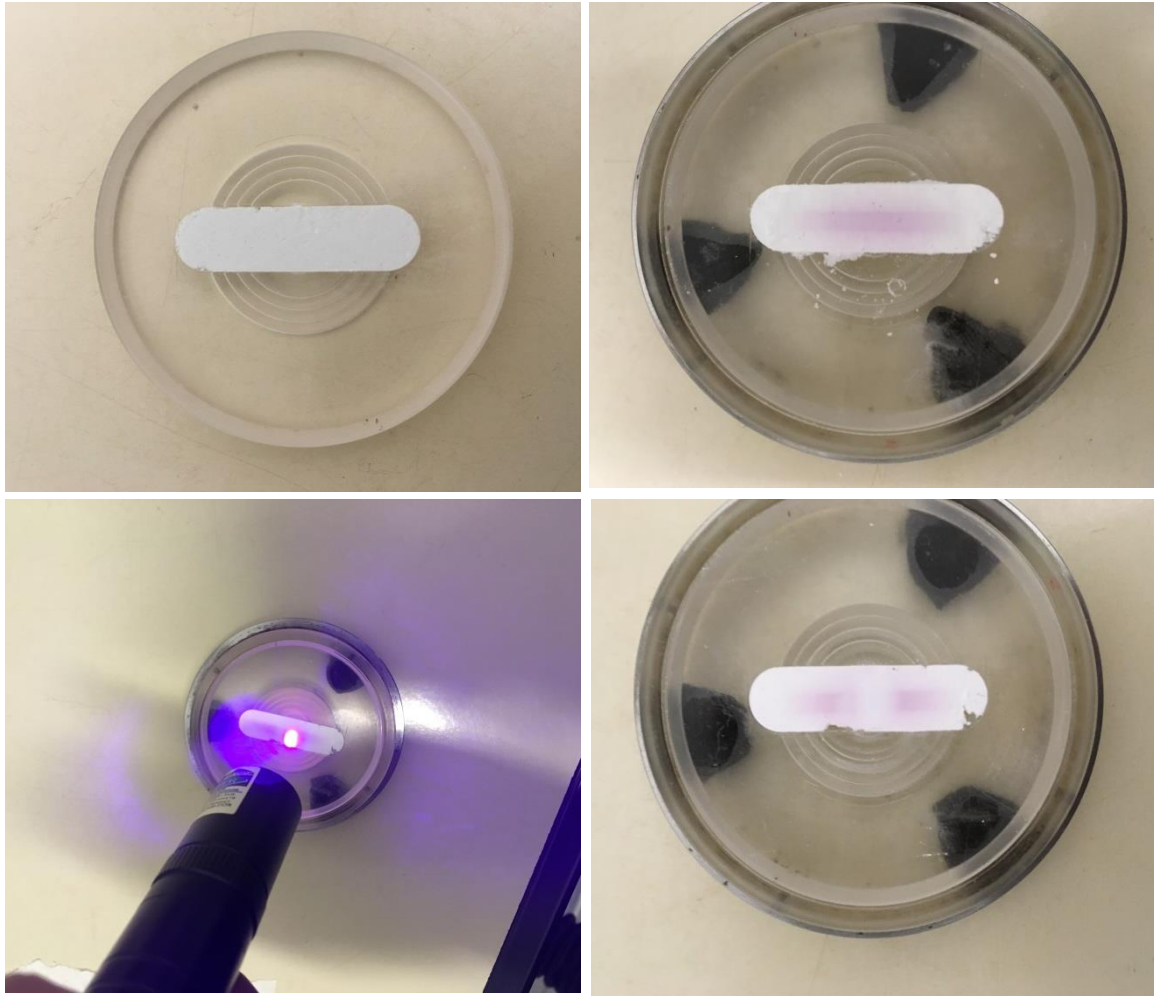


Figure S8. Photochromic response of synthetic hackmanite mineral before and after X-ray ($\text{CuK}\alpha$) radiation exposure for 5 min (top left, and right). Showing the reversibility of the photochromic effect after short time irradiation with a 405 nm laser pointer (bottom).

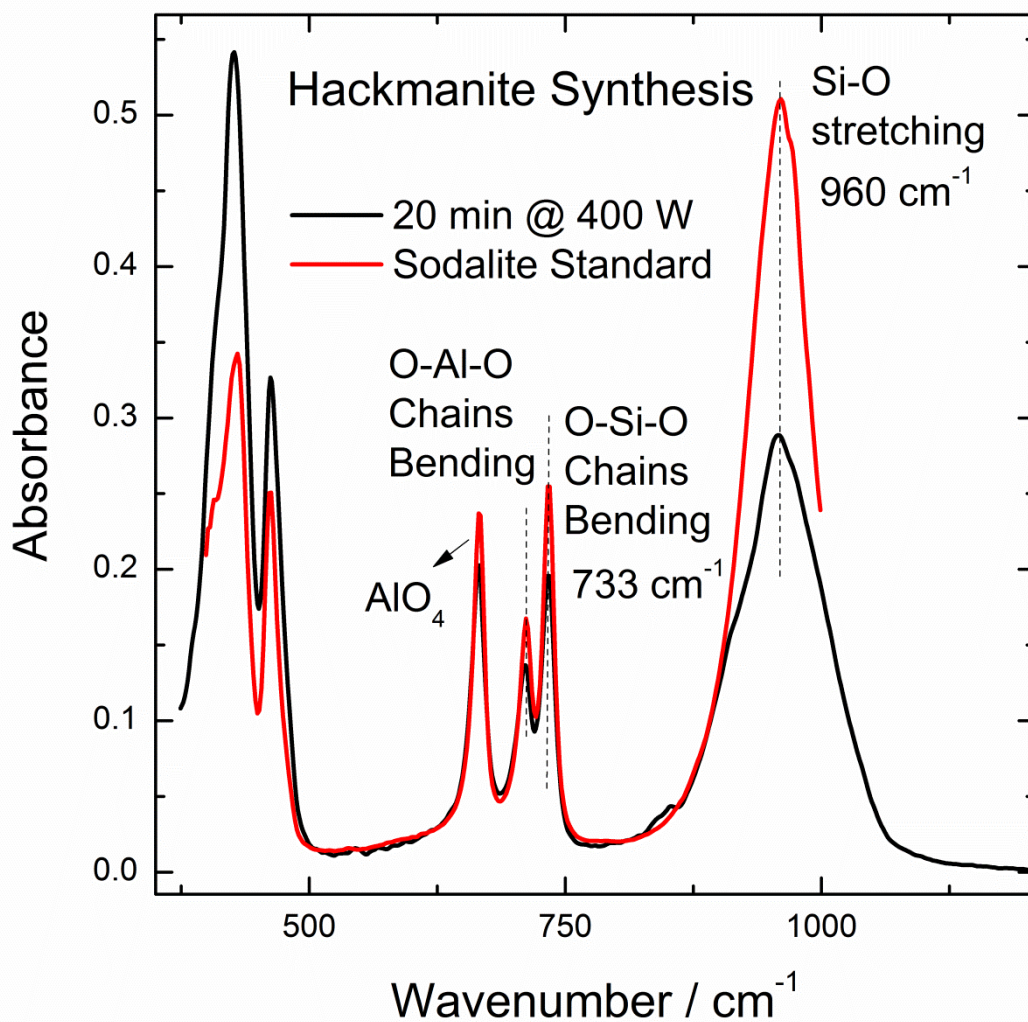


Figure S9. FTIR-ATR absorption spectra of the Na_8 -hackmanite material synthesized after 20 min of microwave irradiation.

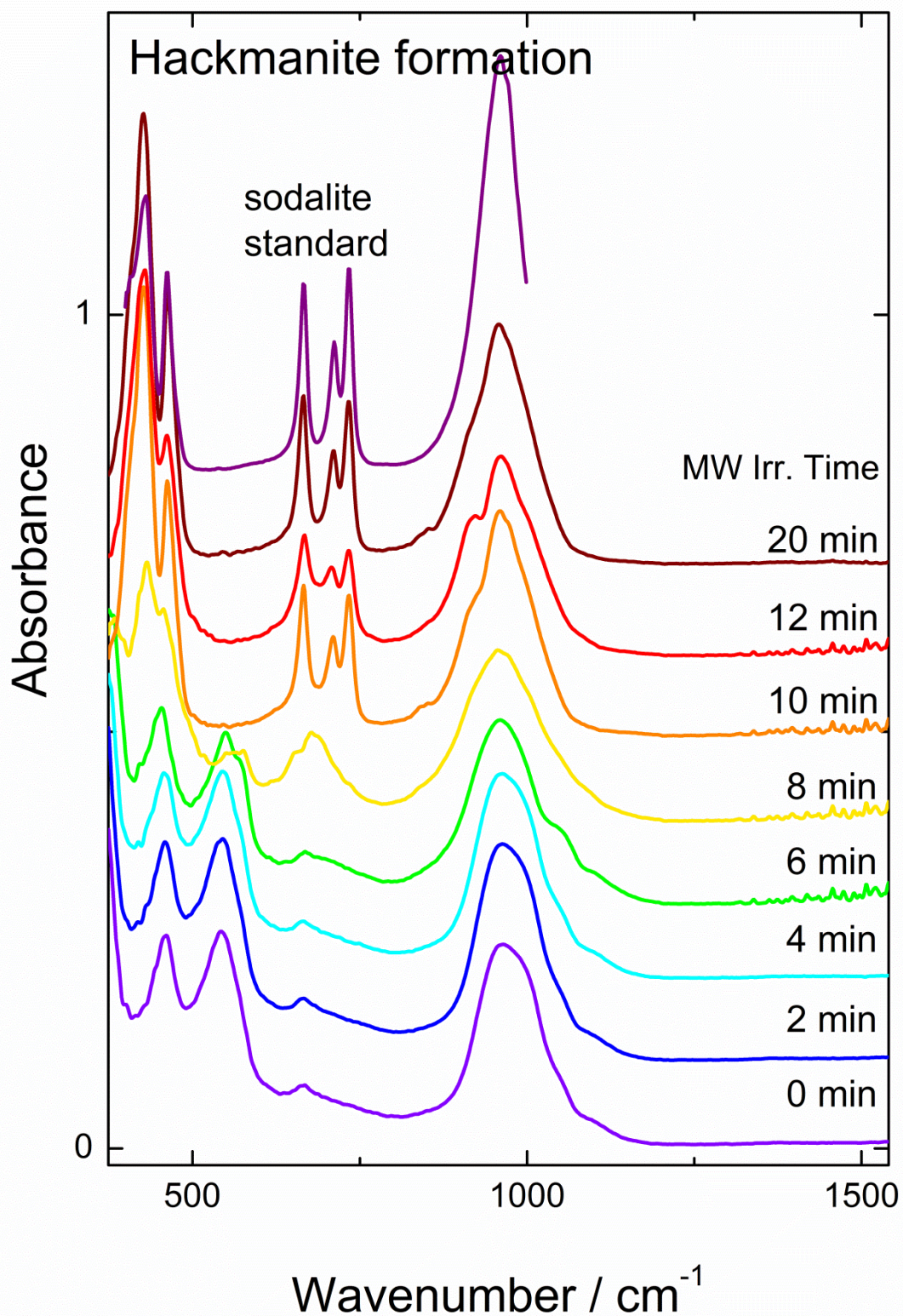


Figure S10. FTIR-ATR absorption spectra of the ex-situ evolution of synthesis of Na-hackmanite material with a 2 minute step of microwave irradiation.

The mechanism of coloration and decoloration in hackmanites is presented in **Fig. S11** below. The mechanism comprises the following six stages³:

- 1) The S_2^{2-} ion absorbs energy ($E > 4$ eV), which causes a photo-induced electron transfer from S_2^{2-} to V_{Cl} thus resulting in $^1[S_2^{\cdot-}, V_{Cl}^{\cdot+}(a_1)]$.
- 2-3) The excited system relaxes geometrically and electronically to a stable triplet state.
- 4) The triplet state absorbs visible light, which causes the purple appearance.
- 5-6) The color can be erased either with optical stimulation (5a) or heating (5b).

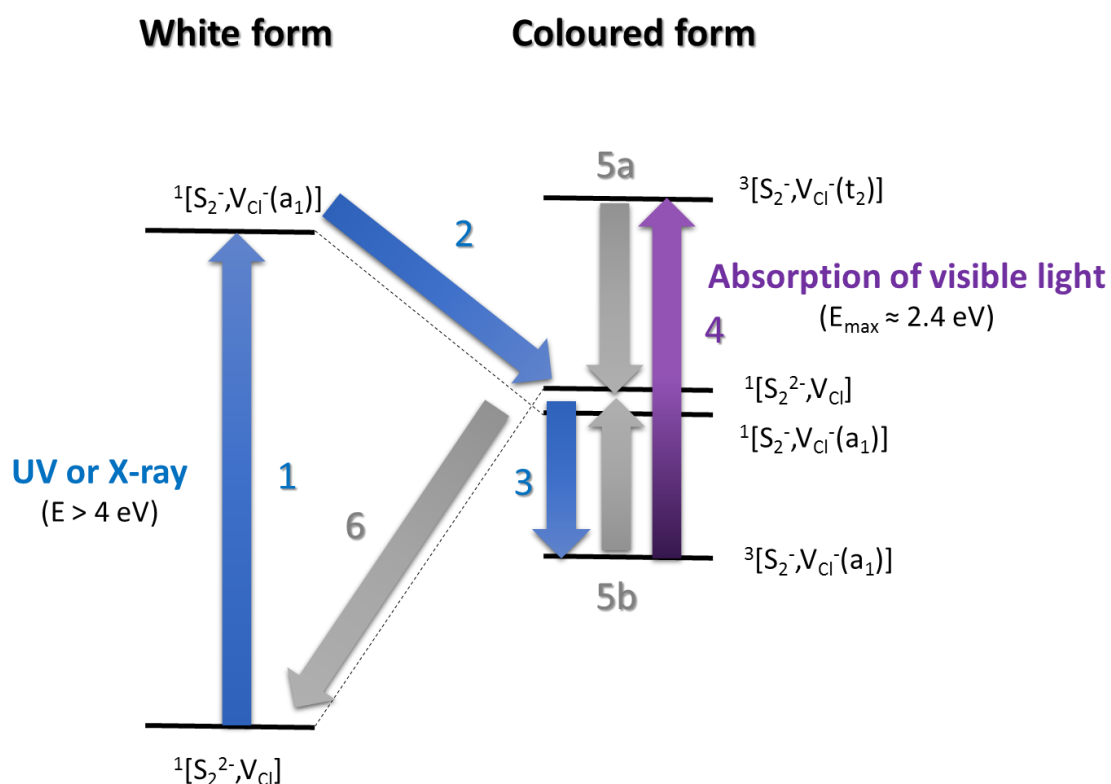


Figure S11. Mechanism for the coloration and decoloration of hackmanites (drawn based on ref 3). The numbers refer to the points discussed above.

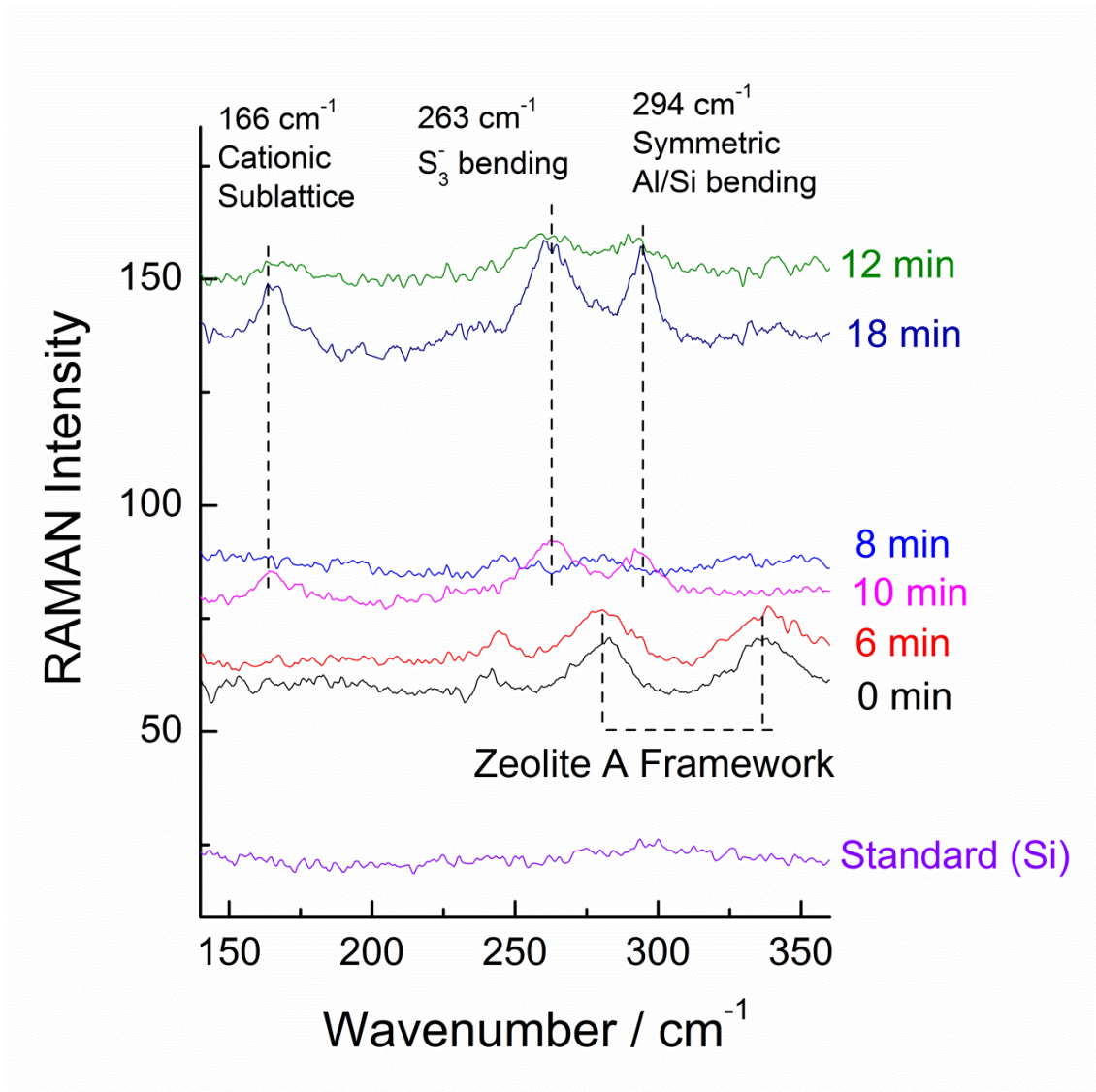


Figure S12. RAMAN spectra (spectral interval: $140\text{-}360 \text{ cm}^{-1}$) of Na-hackmanite material probing *ex-situ* the synthesis evolution using a 2-minutes step of microwave irradiation.

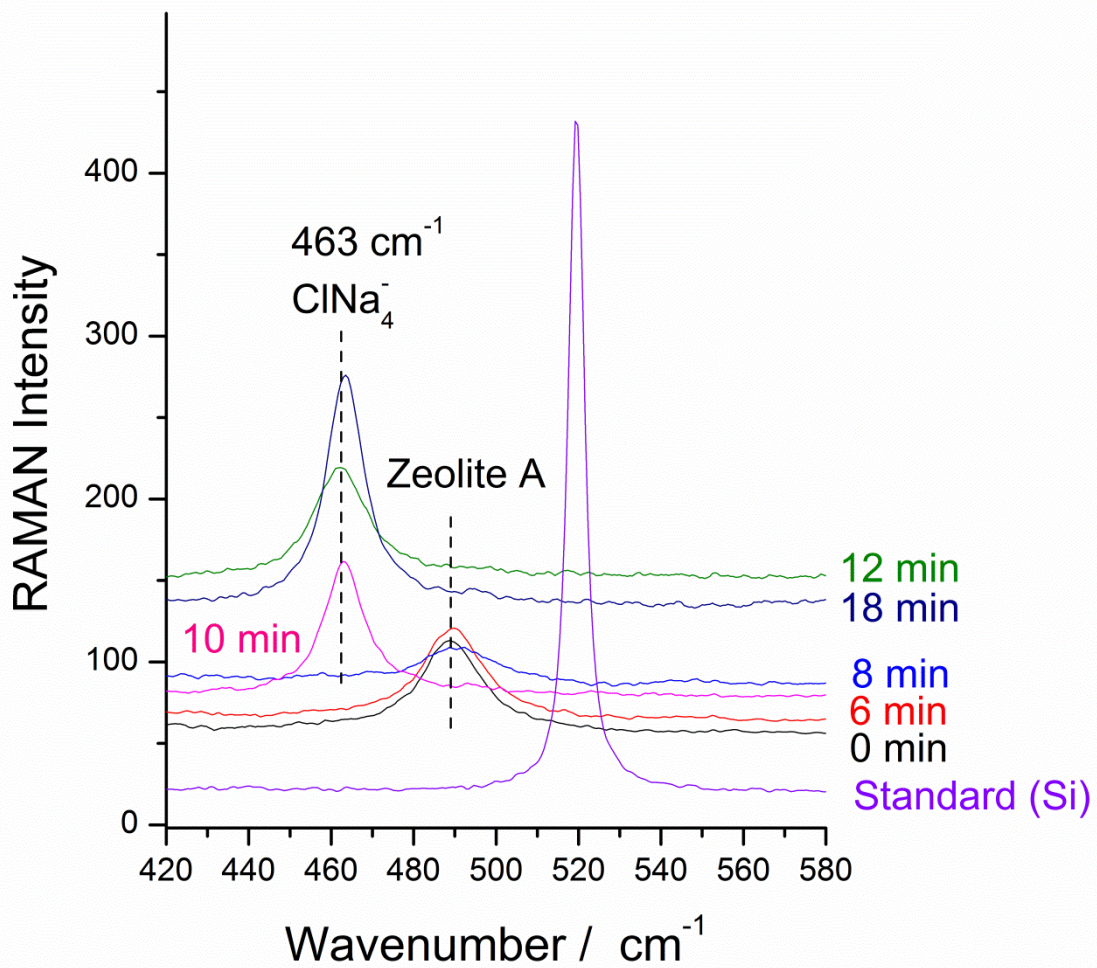


Figure S13. RAMAN spectra (spectral interval: $420\text{-}580 \text{ cm}^{-1}$) of Na-hackmanite material probing *ex-situ* the synthesis evolution using a 2-minutes step of microwave irradiation.

References ESI

- 1 G. B. Dudley, R. Richert and A. E. Stiegman, *Chem. Sci.*, 2015, **6**, 2144–2152.
- 2 J. Hunt, A. Ferrari, A. Lita, M. Crosswhite, B. Ashley and A. E. Stiegman, *J. Phys. Chem. C*, 2013, **117**, 26871–26880.
- 3 I. Norrbo, A. Curutchet, A. Kuusisto, J. Mäkelä, P. Laukkanen, P. Paturi, T. Laihin, J. Sinkkonen, E. Wetterskog, F. Mamedov, T. Le Bahers, and M. Lastusaari, *Mater. Horizons*, 2018, **5** 569-576.